

# Energy-Efficiency and Spectral-Efficiency Trade-off in Distributed Massive-MIMO Networks

Mohd Saif Ali Khan\*, Samar Agnihotri\* and Karthik R.M.†

\*School of Computing & EE, Indian Institute of Technology Mandi, HP, India

†Ericsson India Global Services Pvt. Ltd., Chennai, TN, India

Email: d21013@students.iitmandi.ac.in, samar@iitmandi.ac.in,  
karthik.r.m@ericsson.com

## Abstract

This paper investigates the inherent trade-off between energy efficiency (EE) and spectral efficiency (SE) in distributed massive-MIMO (D-mMIMO) systems. Optimizing the EE and SE together is crucial as increasing spectral efficiency often leads to higher energy consumption. Joint power allocation and AP-UE association are pivotal in this trade-off analysis because they directly influence both EE and SE. We address the gap in existing literature where the EE-SE trade-off has been analyzed but not optimized in the context of D-mMIMO systems. The focus of this study is to maximize the EE with constraints on uplink sum SE through judicious power allocation and AP-UE association, essential for enhancing network throughput. Numerical simulations are performed to validate the proposed model, exploring the impacts of AP-UE association and power allocation on the EE-SE trade-off in uplink D-mMIMO scenarios.

## Index Terms

Distributed Massive MIMO, AP-UE Association, Power Control, Energy & Spectral Efficiency Trade-off

## I. INTRODUCTION

In the era of 5G and beyond, the fast expansion of connected devices and exponential rise in data traffic have made spectral efficiency (SE) and energy efficiency (EE) key network design

factors. Enhanced SE is essential to meet the growing demand for higher data rates and better quality of service, but it often comes at the expense of significantly increased energy consumption due to higher power demands on infrastructure and devices. As the world moves toward green communication to reduce environmental effect, thus establishing the trade-off between the EE and SE becomes a critical challenge in 5G networks, where technologies such as massive MIMO and dense deployment of access points aim to boost SE but risk increasing energy consumption to unsustainable levels, both environmentally and economically. Therefore, striking a balance between SE and EE is not only a technical necessity, but also a critical step towards achieving economically and environmentally sustainable communication systems.

Distributed massive-MIMO (D-mMIMO) combines the advantages of massive-MIMO and the cell-free architecture to improve performance of the network [1]. D-mMIMO systems provide uniform service quality over a large coverage area by distributing antennas across the region, significantly enhancing both EE and SE compared to conventional cellular networks [2].

Interestingly, in general, there is an inherent trade-off between the EE and SE, increasing the SE may eventually lead to a decrease in EE, and vice versa. This trade-off can also be observed in D-mMIMO systems [3]. In [3], the authors have analysed the EE-SE trade-off for downlink scenario, but these EE and SE are not optimized. Power allocation, AP-UE association, and many other factors impact both, the EE and SE of the D-mMIMO [2]. Thus, there is a need to analyse the EE-SE trade-off after performing the optimal resource allocation.

One of the primary factors that influence both EE and SE is power allocation. Another important aspect in D-mMIMO systems is the AP-UE association, where each user is dynamically associated with a subset of APs that collaboratively serve the user. This association plays a vital role in both the EE and SE. Thus, the joint power allocation and AP-UE association is important to enhance the energy and spectral efficiencies of D-mMIMO networks and to analyze their trade-off.

Much work has been done for power allocation and AP-UE association to enhance either SE or EE of the D-mMIMO systems [2], [4]–[11]. But none of the existing work, to the best of our knowledge, deals with the EE-SE trade-off while performing AP-UE association and power allocation for the D-mMIMO.

In this paper, we formulate an optimization problem for EE maximization with a constraint on the quality-of-service (QoS) requirement of the sum SE with respect to power allocation and AP-UE association. The goal is to establish a trade-off between EE and SE while finding the

power allocation across APs and the association between APs and UEs that maximize network performance under these constraints.

*Organization:* The paper is organized as follows: Section II presents the system model highlighting the key components and assumptions used in this study. Section III details the problem formulation. Section IV introduces our proposed solution and establishes its convergence. In Section V, using the proposed solution approach we numerically evaluate the trade-off between the EE and SE with respect to various system parameters. Finally, Section VI concludes our work and provides some directions for future work.

## II. SYSTEM MODEL

We consider a scenario where  $T$  single antenna UEs and  $M$  multi-antenna APs operate within a defined coverage area. Each AP is equipped with  $A$  antennas, and the relationship  $T \ll MA$  indicates a high antenna-to-user ratio, facilitating substantial spatial multiplexing gains. The APs and the UEs are uniformly distributed across the coverage area, ensuring that every UE is within the service range of multiple APs. All APs can serve all UEs simultaneously using the same time and frequency resources. Connectivity between the APs and the central processing unit (CPU) is ensured via a front-haul link, which is critical for coordinating signal processing tasks and distributing user data and control information efficiently across the network as shown in Fig. 1. To ensure network scalability, a user-centric approach has been adopted, where each UE is served by a subset of APs, as depicted in Fig. 1.

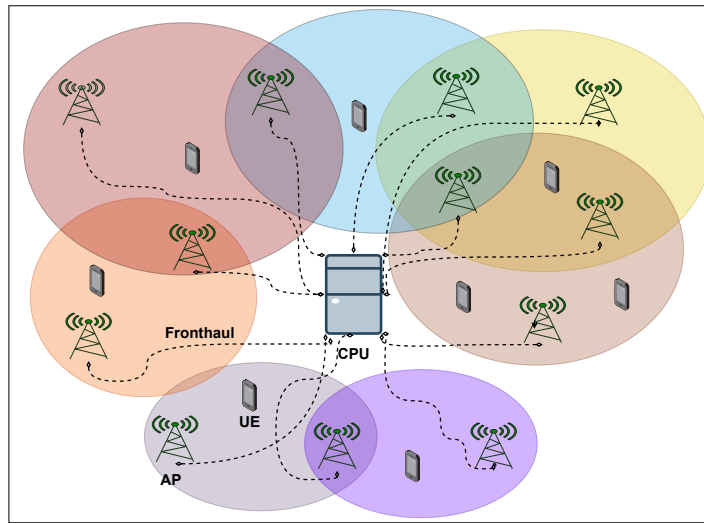


Fig. 1. A typical network model. Here each oval identifies the UE(s) and the APs that serve it(them).

This setup uses Time-Division Duplexing (TDD) mode for communication. Channel estimation is conducted during the uplink phase where the UEs transmit orthogonal pilot signals, and the APs estimate the uplink channel vectors. The system employs a block fading model, characterized by a coherence block of length  $L_c$ . Within each coherence block, a portion defined by  $L_p$  is dedicated to pilot transmission for channel estimation. The small-scale fading component, denoted by  $\mathbf{h}_{mt} \in \mathbb{C}^{A \times 1}$ , follows a Rayleigh distribution. Each component of  $\mathbf{h}_{mt}$  is assumed to be an independent and identically distributed (i.i.d.) complex Gaussian random variable with zero mean and unit variance. Large-scale fading coefficient (LSFC), denoted by  $\beta_{mt}$ , accounts for path-loss and shadowing effects. The overall channel vector  $\mathbf{g}_{mt} \in \mathbb{C}^{A \times 1}$  is given by the product  $\mathbf{g}_{mt} = \beta_{mt}^{1/2} \mathbf{h}_{mt}$ .

### A. Uplink Pilot Training

We assume that during uplink channel estimation, each UE  $t$  transmits the pilot sequence  $\sqrt{L_p} \Psi_t \in \mathbb{C}^{L_p \times 1}$ , such that  $\|\Psi_t\|^2 = 1$ . The received signal  $\mathbf{y}_m^{pilot} \in \mathbb{C}^{A \times L_p}$  is given by :

$$\mathbf{y}_m^{pilot} = \sum_{t=1}^T \sqrt{L_p p_p} \mathbf{g}_{mt} \Psi_t + \mathbf{n}_m,$$

where  $\mathbf{n}_m \in \mathbb{C}^{A \times L_p}$  is the complex additive white Gaussian noise matrix with each element distributed normally with zero mean and unit variance. Also,  $p_p$  represents the normalized signal-to-noise power for pilot transmission. The MMSE estimate  $\hat{\mathbf{g}}_{mt} \in \mathbb{C}^{A \times 1}$  of  $\mathbf{g}_{mt}$  and the mean-square of the estimates are given by [2]:

$$\hat{\mathbf{g}}_{mt} = \frac{\sqrt{L_p p_p} \beta_{mk}}{\sum_{t'=1}^T L_p p_p \beta_{mt'} |\Psi_t^H \Psi_{t'}|^2 + 1} \mathbf{y}_m^{pilot} \Psi_t,$$

$$\gamma_{mt} = \frac{L_p p_p \beta_{mt}^2}{\sum_{t'=1}^T L_p p_p \beta_{mt'} |\Psi_t^H \Psi_{t'}|^2 + 1}.$$

### B. Uplink Data Transmission

The uplink signal received at the  $m^{th}$  AP is given by:

$$\mathbf{y}_m^u = \sqrt{p_u} \sum_{t \in \mathcal{T}} \mathbf{g}_{mt} \sqrt{\eta_t^u} x_t + \mathbf{n}_m,$$

where  $x_t$  is the uplink payload signal transmitted from the UE  $t$ , such that  $\mathbb{E}\{|x_t|^2\} = 1$ . The uplink normalized signal-to-noise power and power control coefficient of the UE  $t$  are denoted

by  $p_u$  and  $\eta^u$ , respectively. The large scale fading decoding (LSFD) of the UE  $t$  for all APs is performed at CPU after local data estimation using the combining vector,  $\mathbf{v}_{mt}$  for APs  $m$ , as :

$$\hat{y}_t = \sum_{m=1}^M d_{mt} \hat{y}_{mt} = \sum_{m=1}^M d_{mt} \mathbf{v}_{mt}^H \mathbf{y}_m^u, \quad (1)$$

where  $d_{mt}$  is the AP-UE association binary variable of the UE  $t$  for AP  $m$  such that when AP  $m$  serves the UE  $t$ , then  $d_{mt} = 1$ , else  $d_{mt} = 0$ . Eq. (1) can be re-written as :

$$\begin{aligned} \hat{y}_t &= \sum_{m=1}^M \sqrt{\eta_t^u p_u} d_{mt} \mathbb{E} \{ \mathbf{v}_{mt}^H \mathbf{g}_{mt} \} x_t + \sum_{m=1}^M \sqrt{\eta_t^u p_u} d_{mt} (\mathbf{v}_{mt}^H \mathbf{g}_{mt} - \mathbb{E} \{ \mathbf{v}_{mt}^H \mathbf{g}_{mt} \}) x_t \\ &+ \sum_{k \in \mathcal{P}_t / \{t\}} \sum_{m=1}^M \sqrt{\eta_t^u p_u} d_{mt} \mathbf{v}_{mt}^H \mathbf{g}_{mk} x_k + \sum_{k \notin \mathcal{P}_t} \sum_{m=1}^M \sqrt{\eta_t^u p_u} d_{mt} \mathbf{v}_{mt}^H \mathbf{g}_{mk} x_k + \sum_{m=1}^M d_{mt} \mathbf{v}_{mt}^H \mathbf{n}_m, \end{aligned}$$

### C. Spectral Efficiency and Energy Efficiency

The uplink spectral efficiency can be given by :

$$\text{SE}_t^u = w \log_2(1 + \Gamma_t), \quad (2)$$

where  $w = (1 - \frac{L_p}{L_c})$  and  $\Gamma_t$  is the effective uplink signal-to-interference-noise ratio (SINR). The closed-form expression of effective SINR for any UE  $t$  the partial full-pilot zero-forcing (PFZF) combining [12] is given by :

$$\Gamma_t = \frac{\eta_t^u p_u \left| \sum_{m \in \mathcal{Z}_t} d_{mt} \gamma_{mt} + A \sum_{m \in \mathcal{Q}_t} d_{mt} \gamma_{mt} \right|^2}{I_t}, \quad (3)$$

where

$$\begin{aligned} I_t &= \mathbf{A}_t^P + \mathbf{B}_t^P + \mathbf{C}_t^P, \\ \mathbf{A}_t^P &= \sum_{t'=1}^T \eta_{t'}^u p_u \left( \sum_{m \in \mathcal{Z}_t} \frac{d_{mt}^2 \gamma_{mt} (\beta_{mt'} - \gamma_{mt'})}{A - L_{S_m}} + A \sum_{m \in \mathcal{Q}_t} d_{mt}^2 \gamma_{mt} \beta_{mt'} \right), \\ \mathbf{B}_t^P &= \sum_{t' \in \mathcal{P}_t / \{t\}} \eta_{t'}^u p_u \left| \sum_{m \in \mathcal{Z}_t} \frac{d_{mt} \gamma_{mt} \sqrt{\eta_{t'}^u} \beta_{mt'}}{\sqrt{\eta_t^u} \beta_{mt}} + A \sum_{m \in \mathcal{Q}_t} \frac{d_{mt} \gamma_{mt} \sqrt{\eta_{t'}^u} \beta_{mt'}}{\sqrt{\eta_t^u} \beta_{mt}} \right|^2, \\ \mathbf{C}_t^P &= \sum_{m \in \mathcal{Z}_t} d_{mt}^2 \frac{\gamma_{mt}}{A - L_{S_m}} + A \sum_{m \in \mathcal{Q}_t} d_{mt}^2 \gamma_{mt}. \end{aligned}$$

The total uplink energy efficiency of the network in bits per joule is defined as:

$$\text{EE} = \frac{wB \sum_{t=1}^T \log_2(1 + \Gamma_t)}{P_T}, \quad (4)$$

where  $B$  is the total bandwidth and according to [13],

$$\begin{aligned} P_T &= P_T^{\text{fix}} + P_T^c + wP_{cpu}^{\text{deco}} B \sum_{t=1}^T \log_2(1 + \Gamma_t), \\ P_T^c &= \sum_{t=1}^T \left( \left( \frac{\eta_t^u p_n p_u}{\zeta} + d_{mt} P_{cpu}^{\text{lsfd}} \right) + \sum_{m=1}^M \left( A d_{mt} P^{\text{proc}} + d_{mt} P^{\text{sig}} \right) \right), \\ P_T^{\text{fix}} &= T P_{ue}^c + M A P_{ap}^c + M P_{fh}^{\text{fix}} + P_{cpu}^{\text{fix}}, \end{aligned}$$

and  $P_{ue}^c$ ,  $P_{ap}^c$ ,  $P^{\text{proc}}$ ,  $P_{fh}^{\text{fix}}$ ,  $P^{\text{sig}}$ ,  $P_{cpu}^{\text{fix}}$ ,  $P_{cpu}^{\text{lsfd}}$  and  $P_{cpu}^{\text{deco}}$  are defined as circuit power of UE, circuit power of the AP, power required for signal processing at the AP, fronthaul linked fix power, signaling power for a fronthaul link, CPU fixed power consumption, power required for LSFd and signal decoding power at the CPU, respectively. Also,  $0 < \zeta \leq 1$  is the power amplifier efficiency and  $p_n$  is the noise power.

### III. PROBLEM FORMULATION

In this section, we introduce an optimization problem formulation for maximizing EE that involves allocating power to all UEs and determining AP-UE allocations, subject to the constraint of achieving a minimum total SE. The problem formulated is given by:

$$\max_{\boldsymbol{\eta}^u, \mathbf{D}} \frac{wB \sum_{t=1}^T \log_2(1 + \Gamma_t)}{P_T^{\text{fix}} + P_T^c + P_{cpu}^{\text{deco}} B \sum_{t=1}^T \text{SE}_t^u}, \quad (5a)$$

$$\text{subject to : } d_{mt} \in \{0, 1\}, \forall m \in \mathcal{M}, t \in \mathcal{T}, \quad (5b)$$

$$0 \leq \eta_t^u \leq 1, \forall t \in \mathcal{T}, \quad (5c)$$

$$w \sum_{t=1}^T \log_2(1 + \Gamma_t) \geq \text{SE}^{\text{QoS}}, \forall t \in \mathcal{T}, \quad (5d)$$

$$\sum_{m=1}^M d_{mt} \geq 1, \forall t \in \mathcal{T}, \quad (5e)$$

where  $\boldsymbol{\eta}^u = \{\eta_t^u\}_{t \in \mathcal{T}}$  and  $\mathbf{D}$  is the AP-UE association matrix with each element as  $d_{mt}$ .  $\mathbf{D}_t$  represents the column vector of matrix  $\mathbf{D}$  with respect to the UE  $t$ . The regularization

coefficient  $\alpha \geq 0$  is the trade-off factor between the front-haul load and the SE.  $SE^{QoS}$  represents the minimum QoS requirement. Constraint (5b) represents the binary variable indicating the association between the UEs and APs. Constraint (5c) represents the uplink power control coefficient. Constraint (5d) is for the minimum QoS requirement and constraint (5e) specifies that at least one AP must be connected to the UE. The above Problem (5) is an instance of mixed-integer non-linear programming (MINLP) problems which are, generally, NP-hard. Thus, to find a solution with lower complexity, we employ the Successive Convex Approximation (SCA) technique [14], as described next.

#### IV. THE SCA BASED ENERGY EFFICIENCY MAXIMIZATION

As argued above, the optimization problem in (5) is, generally, computationally hard. Therefore, in the following we provide an approach to find a feasible solution to this problem that guarantees a predefined system-wise sum SE. The proposed approach employs various relaxations and approximations steps, as outlined and discussed below:

- 1) As both the numerator and denominator of the objective function in (5), we first reformulate the optimization problem to reduce its solution complexity, without affecting the optimality of its solution.
- 2) The MINLP problem is converted into a non-linear programming (NLP) problem by relaxing the binary constraint into continuous constraint.
- 3) The non-linear term inside the logarithm is addressed by introducing auxiliary variables and approximating the non-convex term  $\Gamma_t$  using the quadratic transformation [15], making it tractable.
- 4) The fractional form of the objective function is converted into a tractable form using the auxiliary variables and the quadratic transformation [15].
- 5) The coupling between  $\eta^u$  and  $\mathbf{D}$  introduces non-convexity, which is further handled in the same way as in [11], to ensure the overall problem becomes convex and tractable.
- 6) Finally, an iterative approach is employed to refine the approximated terms towards the original terms, to ensure an accurate solution.

**Step 1:** In the objective function (5a), the numerator and denominator both contain the sum SE term, so instead of maximizing objective function (5a), we maximize new objective function

$\frac{wB \sum_{t=1}^T \log_2(1+\Gamma_t)}{P_T^{\text{fix}} + P_T^c}$ . Then the new problem becomes:

$$\max_{\eta^u, \mathbf{D}} \frac{wB \sum_{t=1}^T \log_2(1 + \Gamma_t)}{P_T^{\text{fix}} + P_T^c}, \quad (6a)$$

$$\text{subject to : } d_{mt} \in \{0, 1\}, \forall m \in \mathcal{M}, t \in \mathcal{T}, \quad (6b)$$

$$0 \leq \eta_t^u \leq 1, \forall t \in \mathcal{T}, \quad (6c)$$

$$w \sum_{t=1}^T \log_2(1 + \Gamma_t) \geq \text{SE}^{\text{QoS}}, \forall t \in \mathcal{T}, \quad (6d)$$

$$\sum_{m=1}^M d_{mt} \geq 1, \forall t \in \mathcal{T}, \quad (6e)$$

As maximizing the objective function (6a) is same as maximizing the original objective function (5a), thus solving Problem (6) is equivalent to solving the original Problem (5).

**Step 2:** We relax the binary variable  $d_{mt}$  to a continuous constraint, as complexity of solving a mixed-integer type problem is exponential. Thus, constraint (6b) can be written as:

$$0 \leq d_{mt} \leq 1, \forall m \in \mathcal{M}, t \in \mathcal{T}. \quad (7)$$

*Remark :* In objective function (6a), the power consumption term behaves as the penalty for the AP-UE association matrix and thus forcing the  $d_{mt}$  to take values either close to one or zero. Thus, maintaining the feasibility of our original constraint (6b).

**Step 3:** Given that  $\Gamma_t$  is a non-linear term inside the logarithmic function, we introduce auxiliary variable  $\Gamma_t^*$  as the lower bound on  $\Gamma_t$ . This substitution removes the non-linearity from the logarithmic term by replacing  $\Gamma_t$  with  $\Gamma_t^*$  in both the objective function (6a) and constraint (6d). Consequently, a new constraint is introduced in Problem (6) to ensure the feasibility of a new variable  $\Gamma_t^*$ . The additional constraint is given as:

$$\Gamma_t^* \leq \Gamma_t, t \in \mathcal{T}. \quad (8)$$

Still, the new constraint (8) is non-convex to fractional non-convex term,  $\Gamma_t$ . Thus, the lower bound of the right hand side of constraint (8) is introduced, by using the quadratic transformation



[15], and is given by:

$$\Gamma_t \geq 2z_t \sqrt{\eta_t^u p_u \left| \sum_{m \in \mathcal{Z}_t} d_{mt} \gamma_{mt} + A \sum_{m \in \mathcal{Q}_t} d_{mt} \gamma_{mt} \right|^2} - z_t^2 I_t, \quad (9)$$

where the optimal value of  $z_t$  is given by:

$$z_t^* = \frac{\sqrt{\eta_t^u p_u \left| \sum_{m \in \mathcal{Z}_t} d_{mt} \gamma_{mt} + A \sum_{m \in \mathcal{Q}_t} d_{mt} \gamma_{mt} \right|^2}}{I_t}. \quad (10)$$

Thus, constraint (8) can be written as, :

$$\Gamma_t^* \leq 2z_t \sqrt{\eta_t^u p_u \left| \sum_{m \in \mathcal{Z}_t} d_{mt} \gamma_{mt} + A \sum_{m \in \mathcal{Q}_t} d_{mt} \gamma_{mt} \right|^2} - z_t^2 I_t. \quad (11)$$

The feasibility of constraint (11) lies in the fact that constraint (11) is the lower bound of constraint (8), as can be seen from inequality (9). Therefore, Problem (6) after incorporating the new auxiliary variable  $\Gamma_t^*$  and constraint (11) becomes:

$$\max_{\eta^u, \mathbf{D}} \frac{wB \sum_{t=1}^T \log_2(1 + \Gamma_t^*)}{P_T^{\text{fix}} + P_T^c}, \quad (12a)$$

$$\text{subject to : } w \sum_{t=1}^T \log_2(1 + \Gamma_t^*) \geq \text{SE}^{\text{QoS}}, \forall t \in \mathcal{T}, \quad (12b)$$

$$(6c), (6e), (7), (11). \quad (12c)$$

In order to solve Problem (12), constraint (11) attempts to achieve equality. The value of  $z_t$  in (11) needs to be updated after each iteration using equation (10). After substitution of  $z_t$  value in (11), constraint (11) becomes equivalent to constraint (8). As the iterations proceeds in our proposed iterative solution,  $\Gamma_t^*$  become equal to  $\Gamma_t$ . This implies that solving Problem (12) is equivalent to solving Problem (6).

**Step 4:** As objective function (12a) is in a fractional form, so to have a more tractable solution, we introduce two new variable  $u$  and  $v$  for the numerator and denominator, respectively. Thus, the new problem becomes:

$$\max_{\eta^u, \mathbf{D}, u, v} \frac{u}{v} \quad (13a)$$

$$\text{subject to : } w \sum_{t=1}^T \log_2(1 + \Gamma_t^*) \geq \text{SE}^{\text{QoS}}, \forall t \in \mathcal{T}, \quad (13b)$$

$$wB \sum_{t=1}^T \log_2(1 + \Gamma_t^*) \geq u, \quad (13c)$$

$$P_T^{\text{fix}} + \bar{P}_T \leq v, \quad (13d)$$

$$(6c), (6e), (7), (11). \quad (13e)$$

Solving Problem (13) is equivalent to solving (12) as constraints (13c) and (13d) must attain equality as iterations proceed. Still, we need to handle the fractional objective function (13a). The objective function (12a), which is a fraction of linear variables can also be approximated using the quadratic transformation [15] as:

$$\frac{u}{v} \geq 2b\sqrt{u} - b^2v, \quad (14)$$

where the optimal value of  $b$  is given by:

$$b^* = \frac{\sqrt{wB \sum_{t=1}^T \text{SE}_t^u}}{P_T^{\text{fix}} + P_T^c}. \quad (15)$$

Since, inequality in (14) provides a lower bound and does not impact the feasibility as maximizing  $2b\sqrt{u} - b^2v$  also maximizes  $\frac{u}{v}$ , thus the new formulation can be written as:

$$\max_{\boldsymbol{\eta}^u, \mathbf{D}, u, v, b, \mathbf{z}, \Gamma^*} 2b\sqrt{u} - b^2v, \quad (16a)$$

$$\text{subject to : } (6c), (6e), (7), (13d), (12b), (11), \quad (16b)$$

where  $\mathbf{z} = \{z_t\}_{t \in \mathcal{T}}$ .

The value of  $b$  in objective function (16a) is updated using equation (15) after each iteration. As the iterations proceeds, objective function (16a) tries to achieve the values same as of objective function (13a). This indicate that solving Problem (16) is equivalent to solving Problem objective function (13).

**Step 5:** After fixing the parameters  $b$  and  $\mathbf{z}$ , the only non-convex term in the above formulation (16) is constraint (11) due to the coupling of  $\boldsymbol{\eta}^u$  and  $\mathbf{D}$ . It should be noted that, the right side of constraint (11) is bi-conacve in  $\boldsymbol{\eta}^u$  and  $\mathbf{D}$ . Thus, Problem (16) can be solved by an alternate optimization technique. First, we fix  $\mathbf{D}$ ,  $b$  and  $\mathbf{z}$ , then solve the following optimization problem:

$$f_1 = \max_{\boldsymbol{\eta}^{\mathbf{u}}, u, v, \boldsymbol{\Gamma}^*} 2b\sqrt{u} - b^2v, \quad (17a)$$

$$\text{subject to : (6c), (13d), (12b), (11).} \quad (17b)$$

After solving Problem (17), we calculate the  $b$  and  $\mathbf{z}$ . Then, we fix the  $\boldsymbol{\eta}^{\mathbf{u}}$ ,  $b$  and  $\mathbf{z}$ , then solve the following optimization problem:

$$f_2 = \max_{\mathbf{D}, u, v, \boldsymbol{\Gamma}^*} 2b\sqrt{u} - b^2v, \quad (18a)$$

$$\text{subject to : (6e), (7), (13d), (12b), (11).} \quad (18b)$$

**Step 6:** After solving Problem (18), we again calculate  $b$  and  $\mathbf{z}$  and then solve Problem (17). The iterative steps in brief are illustrated in the Algorithm 1.

---

**Algorithm 1** Proposed Algorithm

---

- 1: **Feasible Initialization:**  $\boldsymbol{\eta}^{\mathbf{u}(0)}$ ,  $\mathbf{D}^{(0)}$  and  $i = 0$ ,  $\forall t \in \mathcal{T}$ ,  $\epsilon = 5e^{-3}$ .
  - 2: **repeat**
  - 3:      $i = i + 1$ .
  - 4:     **for all**  $t$  **do**
  - 5:         Calculate  $z_t$  using (10).
  - 6:     **end for**
  - 7:     Calculate  $b$  using (15).
  - 8:     Solve optimization problem in (17) for  $\boldsymbol{\eta}^{\mathbf{u}(i)}$ .
  - 9:     **for all**  $t$  **do**
  - 10:         Re-calculate  $z_t$  using (10).
  - 11:     **end for**
  - 12:     Re-calculate  $b$  using (15).
  - 13:     Solve optimization problem in (18) for  $\mathbf{D}^{(i)}$ .
  - 14:     Update  $\boldsymbol{\eta}^{\mathbf{u}(i+1)} = \boldsymbol{\eta}^{\mathbf{u}(i)}$  and  $\mathbf{D}^{(i+1)} = \mathbf{D}^{(i)}$ .
  - 15: **until**  $\left| \frac{f_2^{(i+1)} - f_2^{(i)}}{f_2^{(i)}} \right| \leq \epsilon$ .
- 

*Convergence Analysis :* To demonstrate the non-decreasing nature of the optimization function  $f(\boldsymbol{\eta}^{\mathbf{u}}, \mathbf{D}) = 2b\sqrt{u} - b^2v$ , assume that  $\boldsymbol{\eta}^{\mathbf{u}^*}$  represents the optimal value of  $f$ , when  $\mathbf{D}$  is fixed. Given this, the inequality  $f(\boldsymbol{\eta}^{\mathbf{u}^*}, \mathbf{D}^{(i)}) \geq f(\boldsymbol{\eta}^{\mathbf{u}(i)}, \mathbf{D}^{(i)})$  always holds due to the concavity of the function  $f$  with respect to  $\boldsymbol{\eta}^{\mathbf{u}}$ . When optimizing  $\mathbf{D}$  to  $\mathbf{D}^*$ , with  $\boldsymbol{\eta}^{\mathbf{u}}$  fixed at  $\boldsymbol{\eta}^{\mathbf{u}^*}$ , the inequality  $f(\boldsymbol{\eta}^{\mathbf{u}^*}, \mathbf{D}^*) \geq f(\boldsymbol{\eta}^{\mathbf{u}^*}, \mathbf{D}^{(i)})$  always holds as  $f$  is concave with respect to  $\mathbf{D}$ . Therefore, combining these observations, we see that  $f(\boldsymbol{\eta}^{\mathbf{u}(i+1)}, \mathbf{D}^{(i+1)}) \geq f(\boldsymbol{\eta}^{\mathbf{u}(i)}, \mathbf{D}^{(i)})$ , indicating  $f$  is non-decreasing

at each iteration. This non-decreasing trend makes the optimization function monotonically increasing in each iteration and also the optimization function is bounded from above, ensuring the convergence of the optimization algorithm, as the function does not increase indefinitely but plateaus at the maximum value.

## V. NUMERICAL SIMULATIONS

We conduct numerical simulations over a geographic area of  $1 \times 1$  square kilometer with APs and UEs distributed randomly. To emulate an infinitely large network, we employ a wrap-around topology as described in [8]. The large-scale fading coefficients follow a three-slope path loss model, with shadow fading modeled by an 8 dB standard deviation. In our simulations, we fix  $T = 30$ ,  $M = 40$ ,  $A = 8$ ,  $L_c = 200$ , and  $L_p = 5$ . Unless explicitly mentioned otherwise, other parameters remain consistent with those in [2]. We average the numerical results across 100 simulation runs.

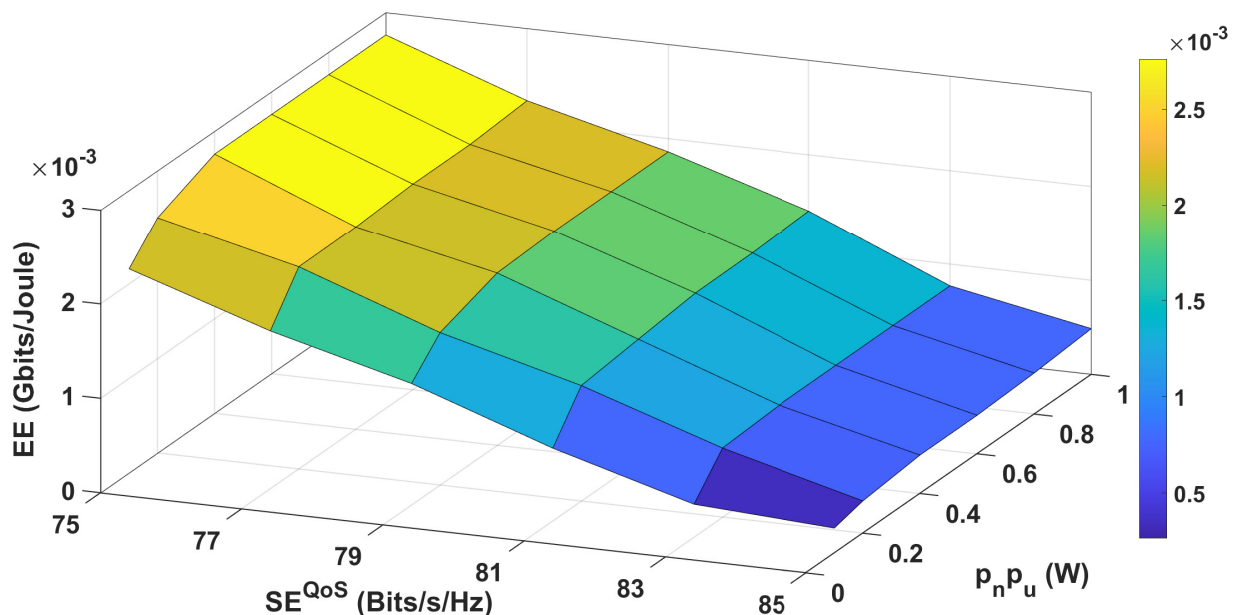


Fig. 2. The EE versus the sum SE threshold versus the maximum power level.

Fig. 2 represents the 3-D plot between the EE, the sum SE threshold and the maximum uplink power ( $p_n p_u$ ) that UEs can attain. In this plot, the sum SE threshold varies from 75 to 85 Bits/s/Hz, and the maximum uplink UE power is varied from 0.1 to 1 W. For the maximum power level of 0.1 W, EE decreases from  $2.16 \times 10^{-3}$  to  $2.64 \times 10^{-4}$  Gbits/Joule as the  $SE^{QoS}$  increases

from 75 to 85 Bits/s/Hz. A similar trend is observed at a power level of 0.2 W, the EE reduces from  $2.5 \times 10^{-3}$  to  $3.42 \times 10^{-4}$  Gbits/Joule for the same increase in  $SE^{QoS}$ . This decreasing pattern persists across higher power levels from 0.4 to 1 W, consistently showing a reduction in EE as  $SE^{QoS}$  increases. This decline is attributed to the necessity of either allocating more APs to UEs, increasing the power allocated to UEs, or both, to enhance the SE. Consequently, this increases the overall power consumption and diminishes the network's EE. We note an increase in the EE with rising maximum uplink power up to a certain point for the fixed sum SE threshold. Notably, the EE begins to saturate beyond a power level of 0.4 W for lower  $SE^{QoS}$ . The optimization algorithm, thereby, increases power consumption only when it contributes to the enhanced EE. For, the higher  $SE^{QoS}$ , however, the EE continues to increase with the rise in maximum power level, indicating that higher power levels contribute more significantly to achieving higher SE.

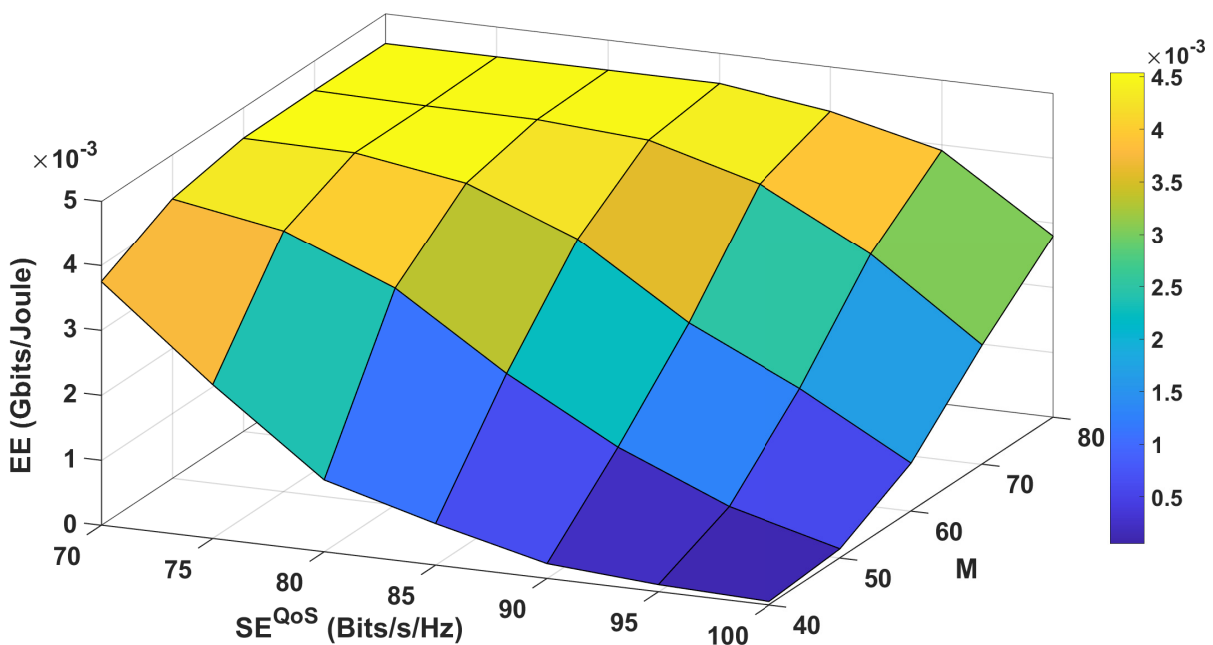


Fig. 3. The EE versus the sum SE threshold versus number of APs for  $p_n p_u = 0.1$ .

Fig. 3 represents the 3-D plot between the EE, sum SE threshold and number of APs ( $M$ ). For  $M = 40$ , the EE decreases from  $3.75 \times 10^{-3}$  to  $5.49 \times 10^{-5}$  Gbits/Joule as the  $SE^{QoS}$  increases from 70 to 100 Bits/s/Hz. A similar trend is observed at  $M = 80$ , the EE declines from  $4.53 \times 10^{-3}$  to  $2.8 \times 10^{-3}$  Gbits/Joule for the same increase in  $SE^{QoS}$ . This decreasing pattern persists as the number of APs increases to 80 from 40, consistently showing a reduction

in the EE as  $SE^{QoS}$  rises. This consistent decrease across AP configurations indicates that higher spectral efficiency necessitate more power per unit of data transmitted, thereby reducing the EE. For the fixed  $SE^{QoS}$ , we observe an increase in the EE with the increase in the number of APs. This indicates that the rate of increase in the SE is more than the rate of increase in circuit power due to the increase in the number of APs. However, this increase is modest at lower  $SE^{QoS}$  values such as 70 and 75 Bits/s/Hz. For the lower values of  $M$ , the optimization algorithm is easily able to achieve these lower  $SE^{QoS}$  values without allocating more APs to UEs, thus not increasing the power consumption. For higher values of  $M$ , due to increase in the circuit power, the total power consumption increases. However, with more APs, the likelihood of having APs closer to UES increases, resulting in stronger channel condition. This proximity enhances both the SE and the EE by offsetting the impact of increases circuit power. For the higher  $SE^{QoS}$  values, when the number of APs are low, in order to maintain the high sum SE, the optimization algorithm allocate more APs to UEs, thus significantly reducing the EE due to increase in power consumption. However, when the number of APs is larger for these higher  $SE^{QoS}$  values, the optimizing algorithm allocates fewer APs per UEs, hence reducing the power consumption and thus enhancing the EE.

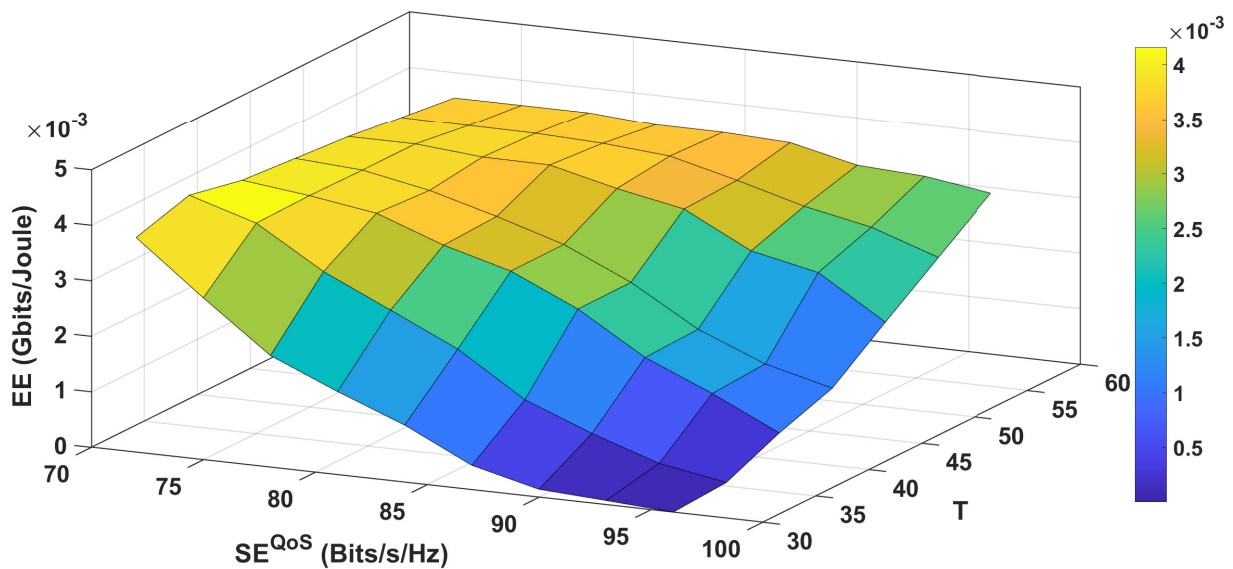


Fig. 4. The EE versus the sum SE threshold versus number of UEs for  $p_n p_u = 0.1$ .

Fig. 4 represents the 3-D plot between the EE, the sum SE threshold and number of UEs ( $T$ ). For a fixed  $T$ , an increase in the  $SE^{QoS}$  leads to a decline in EE. At lower  $SE^{QoS}$  values, the

EE initially increases with  $T$  but eventually decreases when  $T$  becomes very high. This decline is attributed to the increased circuit power consumption required to accommodate more users at lower  $SE^{QoS}$  values. Conversely, at higher  $SE^{QoS}$  values, the EE consistently improves as a larger number of UEs facilitates achieving these higher  $SE^{QoS}$  values.

## VI. CONCLUSION AND FUTURE WORK

This work has systematically explored the complex relationships among energy efficiency, spectral efficiency, and resource allocation parameters such as the number of APs and uplink power levels in distributed massive-MIMO (D-mMIMO) systems. A consistent trade-off between EE and SE is evident across different system configurations and parameters. As the SE demands increase, the EE generally decreases, indicating that higher data transmission rates necessitate greater power expenditure. This work also indicates the role of power allocation and the AP-UE association to achieve desired SE, while maintaining the satisfactory EE. The insights from this study underscore the necessity for sophisticated resource allocation strategies that prioritize both EE and SE, which is especially crucial in the era of 5G and 5G Advanced technologies. These technologies, generally, enhance SE but increase power consumption as well, making the study of this trade-off essential to maintain the environmental and the economic sustainability.

A compelling future direction would involve drawing detailed comparisons of the EE-SE trade-offs across different network architectures, including small-cell networks, traditional mMIMO and the D-mMIMO. Additionally, the influence of modulation and coding schemes, which is not considered in this study, presents an interesting direction for further exploration.

## REFERENCES

- [1] M. S. A. Khan, S. Agnihotri, and R. Karthik, "Distributed pilot assignment for distributed massive-MIMO networks," in *Proc. IEEE WCNC*, Dubai, UAE, April 2024.
- [2] H. Q. Ngo, A. Ashikhmin, H. Yang, E. G. Larsson, and T. L. Marzetta, "Cell-free massive MIMO versus small cells," *IEEE Trans. on Wireless Commun.*, vol. 16, no. 3, pp. 1834–1850, 2017.
- [3] Y. Huang, Y. Jiang, F.-C. Zheng, P. Zhu, D. Wang, and X. You, "Performance of spectral and energy efficiency in cell-free massive MIMO-aided URLLC system with short blocklength communications," *IEEE Trans. on Veh. Techno.*, vol. 73, no. 9, pp. 13,023–13,037, 2024.
- [4] H. Q. Ngo, L.-N. Tran, T. Q. Duong, M. Matthaiou, and E. G. Larsson, "On the total energy efficiency of cell-free massive MIMO," *IEEE Trans. on Green Commun. and Network.*, vol. 2, no. 1, pp. 25–39, 2017.
- [5] T. X. Vu, S. Chatzinotas, S. ShahbazPanahi, and B. Ottersten, "Joint power allocation and access point selection for cell-free massive MIMO," in *Proc. IEEE ICC*, Online, June 2020.

- [6] H. Q. Ngo, H. Tataria, M. Matthaiou, S. Jin, and E. G. Larsson, "On the performance of cell-free massive MIMO in Ricean fading," in *Proc. IEEE ACSSC*, Pacific Grove, CA, USA, Oct. 2018.
- [7] M. Guenach, A. A. Gorji, and A. Bourdoux, "Joint power control and access point scheduling in fronthaul-constrained uplink cell-free massive MIMO systems," *IEEE Trans. on Commun.*, vol. 69, no. 4, pp. 2709–2722, 2020.
- [8] E. Björnson and L. Sanguinetti, "Scalable cell-free massive MIMO systems," *IEEE Trans. on Commun.*, vol. 68, no. 7, pp. 4247–4261, 2020.
- [9] T. C. Mai, H. Q. Ngo, and L.-N. Tran, "Energy efficiency maximization in large-scale cell-free massive MIMO: A projected gradient approach," *IEEE Trans. on Wireless Commun.*, vol. 21, no. 8, pp. 6357–6371, 2022.
- [10] C. Hao, T. T. Vu, H. Q. Ngo, M. N. Dao, X. Dang, C. Wang, and M. Matthaiou, "Joint user association and power control for cell-free massive MIMO," *IEEE Internet of Things Journal*, vol. 11, no. 9, pp. 15 823–15 841, 2024.
- [11] M. S. A. Khan, S. Agnihotri *et al.*, "Joint AP-UE association and power factor optimization for distributed massive MIMO," *arXiv preprint arXiv:2402.14693*, 2024.
- [12] J. Zhang, J. Zhang, E. Björnson, and B. Ai, "Local partial zero-forcing combining for cell-free massive MIMO systems," *IEEE Trans. on Commun.*, vol. 69, no. 12, pp. 8459–8473, 2021.
- [13] S. Chen, J. Zhang, E. Björnson, Ö. T. Demir, and B. Ai, "Sparse large-scale fading decoding in cell-free massive MIMO systems," in *Proc. IEEE SPAWC*, Oulu, Finland, July 2022.
- [14] M. Razaviyayn, "Successive convex approximation: Analysis and applications," Ph.D. dissertation, University of Minnesota, 2014.
- [15] K. Shen and W. Yu, "Fractional programming for communication systems—part II: Uplink scheduling via matching," *IEEE Trans. on Signal Processing*, vol. 66, no. 10, pp. 2631–2644, 2018.